Spatiotemporal Variations of Cloud Amount over the Yangtze River Delta, China

ZHAO Wenjing (赵文静), ZHANG Ning* (张 宁), and SUN Jianning (孙鉴泞)

Institute for Climate and Global Change Research and School of Atmospheric Sciences, Nanjing University, Nanjing 210093

(Received September 2, 2013; in final form February 15, 2014)

ABSTRACT

Based on the NOAA's Advanced Very High Resolution Radiometer (AVHRR) Pathfinder Atmospheres Extended (PATMOS-x) monthly mean cloud amount data, variations of annual and seasonal mean cloud amount over the Yangtze River Delta (YRD), China were examined for the period 1982–2006 by using a linear regression analysis. Both total and high-level cloud amounts peak in June and reach minimum in December, mid-level clouds have a peak during winter months and reach a minimum in summer, and low-level clouds vary weakly throughout the year with a weak maximum from August to October. For the annual mean cloud amount, a slightly decreasing tendency (–0.6% sky cover per decade) of total cloud amount is observed during the studying period, which is mainly due to the reduction of annual mean high-level cloud amount (–2.2% sky cover per decade). Mid-level clouds occur least (approximately 15% sky cover) and remain invariant, while the low-level cloud amount shows a significant increase during spring (1.5% sky cover per decade) and summer (3.0% sky cover per decade). Further analysis has revealed that the increased low-level clouds during the summer season are mainly impacted by the local environment. For example, compared to the low-level cloud amounts over the adjacent rural areas (e.g., cropland, large water body, and mountain areas covered by forest), those over and around urban agglomerations rise more dramatically.

Key words: cloud amount, PATMOS-x, Yangtze River Delta

Citation: Zhao Wenjing, Zhang Ning, and Sun Jianning, 2014: Spatiotemporal variations of cloud amount over the Yangtze River Delta, China. *J. Meteor. Res.*, **28**(3), 371–380, doi: 10.1007/s13351-014-3064-0.

1. Introduction

Clouds are a crucial factor in local and regional climate change. They modulate the earth's radiation budget and the hydrologic cycle (Randall and Tjemkes, 1991). Meanwhile, different cloud types always produce different climate effects and can also reflect different atmospheric conditions. Thus, it is important to investigate the long-term change not only in total clouds but also in different cloud types.

In recent decades, many observational studies have focused on the analyses of clouds over China. Using surface observations, Kaiser (1998) found a decrease in the annual mean total cloudiness over China between 1951 and 1994. Li et al. (2004) studied the spatial distribution and seasonal variation of different types of clouds over China based on the ISCCP (International Satellite Cloud Climatology Project) satellite data and surface observations from 1990 to 1998. Endo and Yasunari (2006) examined the long-term trends of the low-level cloud frequencies and low-level cloud amounts over China with surface observations from 1971 to 1996. At the same time, much attention has also been paid to the relationships between the spatiotemporal variation of clouds and other climate parameters. Kaiser (2000) discussed the relationship between the total cloudiness and other meteorological variables over China, including station pressure, relative humidity, and water vapor pressure. Liang and Xia (2005) and Qian et al. (2006) pointed out that decreasing trends are found in both the cloudiness and solar radiation over China, and the cause for decreas-

Supported by the National Basic Research and Development (973) Program of China (2010CB428501) and National Natural Science Foundation of China (41375014).

*Corresponding author: ningzhang@nju.edu.cn.

ing radiation over China is probably increasing aerosols but not cloudiness. Warren et al. (2007) analyzed the variations of cloudiness and cloud types based on surface observations from 1971 to 1996, and discussed the anthropogenic influence on clouds. They considered the effect of smoke aerosols on cloud amount nonnegligible.

Though many previous studies have focused on cloud amount or cloud frequency over all of China, this paper focuses on a specific area, the Yangtze River Delta (YRD), China. YRD is the largest urban agglomeration area in China (Fig. 1b), which covers an area of 110800 km^2, with a population of more than 97 million. With rapid urbanization, a series of human activities have likely caused local climate change in this area, such as the urban heat island (UHI) effect (Zhang N. et al., 2010) and changes in solar radiation absorption (Zhang et al., 2004). Few investigations have tried to research long-term cloud changes over this area, although clouds are closely related to the surface energy balance, solar radiation, precipitation, and so on. This study analyzes the spatiotemporal characteristics of multi-layered cloud amounts over the YRD, by using the NOAA's Advanced Very High Resolution Radiometer (AVHRR) Pathfinder Atmospheres Extended (PATMOS-x) monthly average cloud amount records from 1982 to 2006.

2. Data and methods

The NOAA-AVHRR PATMOS-x is a project to derive long-term surface and atmospheric climate records (cloud, aerosol, surface, and radiometric) from roughly 30 yr of data from NOAA's AVHRR (including AVHRR/2 and AVHRR/3) onboard the Polar Operational Enrironmental Satellite (POES) spacecraft from 1981 to present. The POES system includes a morning satellite with equator crossing times at approximately 0700 (descending orbit) and 1900 (ascending orbit) local solar time (LST), and an afternoon satellite with the equator crossing times at approximately 0200 (descending orbit) and 1400 (ascending orbit) LST, thus providing global coverage 4 times a day. From the average of all data from afternoon and morning satellite retrievals, an approximate daily and monthly mean is calculated. Monthly averaged cloud amount data retrieved from PATMOS-x version 4 with a 0.5-degree spatial resolution are analyzed in this study, and the cloud types are defined by the cloud-top pressure (Rossow and Schiffer, 1999) as shown in Table 1. Note that before 1992 there was no morning data included in PATMOS-x, so the monthly averaged cloud amounts are simply the average of the afternoon satellite records before 1992. A comparison between the data from only the afternoon satellite observations

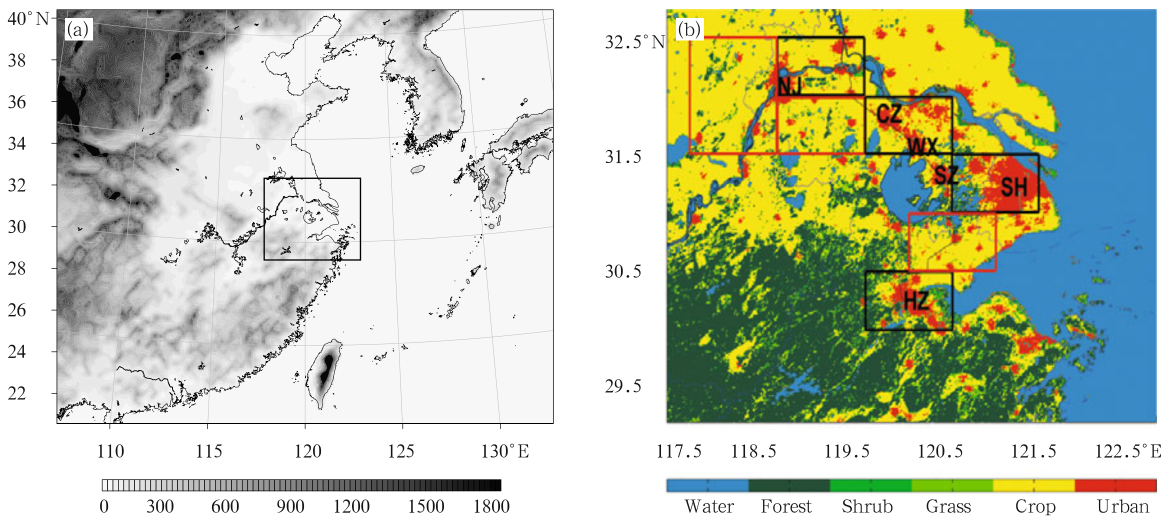

Fig. 1. (a) Topographic height and the analysis area (the black rectangle enclosed area). (b) Land covers in the analysis area, from MODIS observations in 2005. The black and red rectangular areas indicate urban area and cropland area, respectively, which are also mentioned in Fig. 6. NJ: Nanjing; CZ: Changzhou; WX: Wuxi; SZ: Suzhou; SH: Shanghai; HZ: Hangzhou.

Table 1. The cloud types defined by cloud-top pressure

Cloud types	Cloud-top pressure
High-level cloud	Less than 440 hPa
Mid-level cloud	Between 440 and 680 hPa
Low-level cloud	Greater than 680 hPa

and both morning and afternoon observations during 1992–2006 (Fig. 2) shows that the observations from two satellites and one afternoon satellite consist well on the variations of the annual mean data series, although there is a bias of 1%–3% sky cover in cloud amount. Similar characteristics are also found in four seasons (figure omitted). In order to consider a longer observation series, the whole time series of cloud amount (1982–2006) are examined and analyzed in this paper, and the differences between the datasets before and after 1992 are considered as an intervention impact on the trend detection (Weatherhead et al., 1998).

The Clouds from AVHRR Extended (CLAVR-x) algorithms are used to detect PATMOS-x clouds (Pavolonis and Heidinger, 2004; Pavolonis et al., 2005; Heidinger and Pavolonis, 2009). The global cloud amounts from CLAVR-x agree well with other established satellite-derived cloud climatologies (Thomas et al., 2004), and have been widely used in current research of cloud changes (Clement et al., 2009; Tang et al., 2012). It should be noticed that there are some limitations in passive remote sensing observations compared with the active remote sensing (Kennedy et al., 2010; Xi et al., 2010). For the CLVAR-x approaches that can estimate opaque clouds well, there is difficulty in uniquely detecting thin cirrus and small clouds (not filling the sensor field of view) (Nieman et al., 1993; Heidinger and Pavolonis, 2009). However, the approaches can detect multilayered cloud only in situations where thin and high clouds are situated over low, thick clouds (Pavolonis

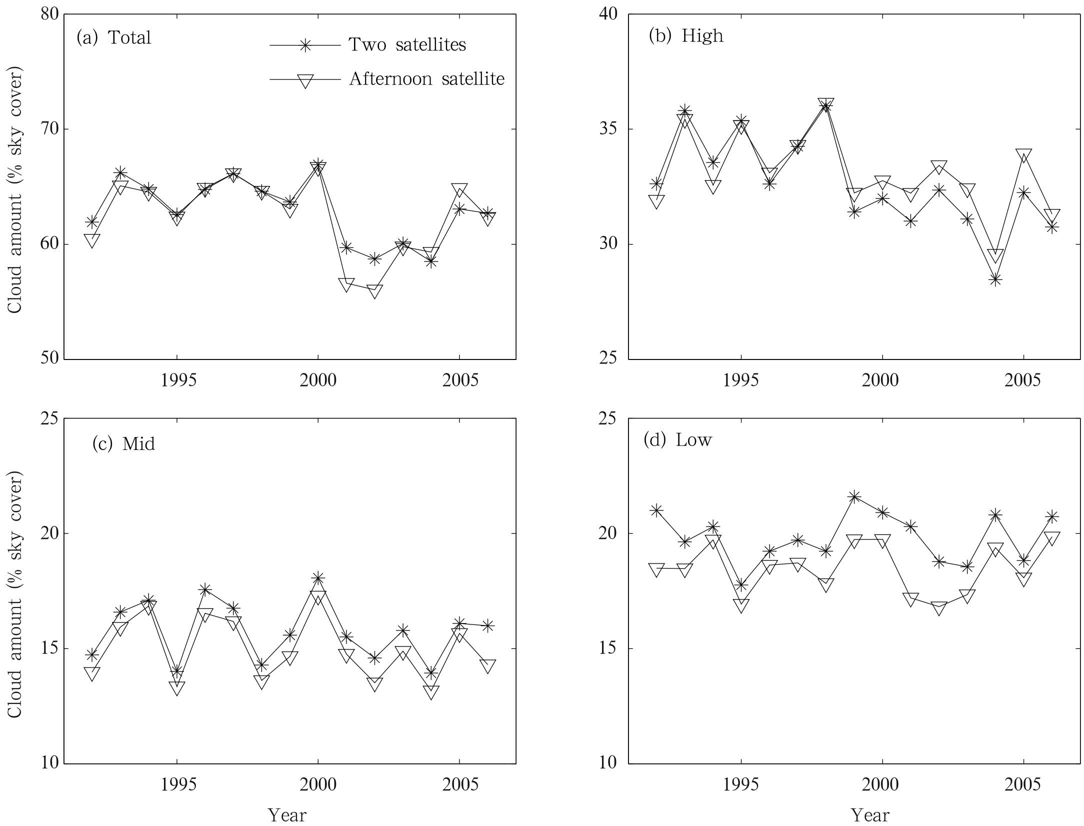

Fig. 2. Annual mean cloud amounts (% sky cover) of (a) total cloud, (b) high-level cloud, (c) mid-level cloud, and (d) low-level cloud, from both morning and afternoon satellites retrievals (line with asterisks) and from only the afternoon satellite retrievals (line with triangles).

and Heidinger, 2004). This paper focuses on the trends/tendencies of cloud amounts rather than the accurate cloud amount values when considering the uncertainties in observation methods.

In this study, a linear regression analysis is performed to analyze the variation in cloud. Tiao et al. (1990) and Weatherhead et al. (1998) pointed out that the precision of linear trend estimate is strongly influenced by the autocorrelation of the noise and intervention in the data series, such as when an instrument is changed at a specific time. Given that there is a permanent shift in the data series in 1992, we consider a trend model as follows (Weatherhead et al., 1998).

$$Y_t = a + bX_t + cU_t + N_t,$$

where $t = 1, 2, \cdots, T$ ($T = 25$ is the number of years); Y_t is the cloud amount series; $X_t = 1982, 1983, \cdots, 2006$; a is a constant term; b is the trend; cU_t is a mean level shift term accounting for the intervention impact at the specific time $t = T_0$ (in this study $T_0 = 11$, corresponding to $X_t = 1992$): $U_t = 0$ ($t < T_0$), $U_t = 1$ ($t \geqslant T_0$). The noise term N_t is assumed as a first-order autoregressive [AR(1)]: $N_t = \rho N_{t-1} + \varepsilon_t$, where ρ is the autocorrelation coefficient and ε_t is the white noise with mean zero and common variance. Regression coefficients a, b, and c are estimated by the method of generalized least squares (GLS) and detailed processes and corresponding discussions were presented well in Weatherhead et al. (1998).

A commonly used criterion is adopted to test the significance of trends: a real trend is indicated at the 95% confidence level when $\mid \hat{b}/\sigma_{\hat{b}} \mid > 2$, where $\hat{b}$ is the estimator of b and $\sigma_{\hat{b}}$ is the uncertainty of trend estimate (standard deviation of $\hat{b}$). It is found that the trend estimate and its uncertainty are strongly influenced by the level shift term in the trend model. The level shift term will not only increase the uncertainty of the trend estimate but also modify its value: $\hat{b} \approx \hat{b}_0 - \hat{c}(6\tau(1-\tau)/T)$, where $\tau = (T_0 - 1)/T$, $\hat{c}$ is the estimator of c, and $\hat{b}_0$ is the trend estimate in the trend model without considering the level shift term ($c = 0$). In addition, the confidence level ($|\hat{b}/\sigma_{\hat{b}}|$) is substantially reduced when including the level shift term in the trend model.

Low-level clouds should be more sensitive to local land surface conditions than higher clouds. Thus, we focus on the time-space distributions of the low-level cloud amount in summer and try to examine if land-surface heterogeneity has any influence on local clouds.

3. Results

The monthly variations of cloud amounts are illustrated in Fig. 3. The total cloud amount peaks in June and then gradually decreases from summer to winter with a minimum in December. High-level clouds occur most frequently from March to October and have a similar monthly variation with total clouds. The mid-level cloud amount peaks during the winter months and reaches a minimum in summer. The variation of low-level clouds is weak and the value from August to October is slightly greater than the other months.

Annual and seasonal changes of cloud amounts averaged over the YRD are analyzed by using the linear regression analysis (Fig. 4). Here, trends are considered statistically significant when the confidence interval is greater than 95%; otherwise, the temporal variations are considered as tendencies (Dong et al., 2010). For the annual mean cloud amounts (Fig. 4a), the averages of total and high-, mid-, and low-level cloud amounts during the studying period are 63%, 32%, 15%, and 19%, respectively. The annual mean total clouds increased in the 1980s, peaked in the 1990s, and then dramatically decreased in 2000,

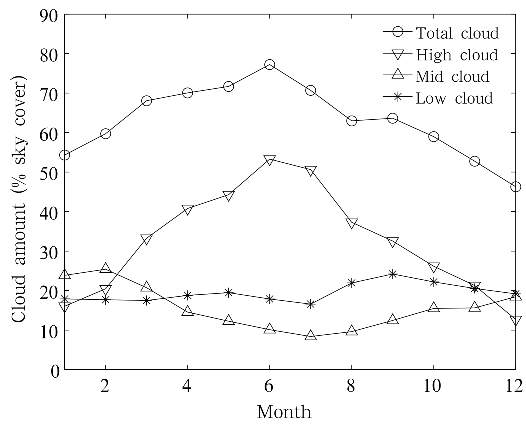

Fig. 3. Monthly mean cloud amounts during the period 1982–2006, averaged over the Yangtze River Delta.

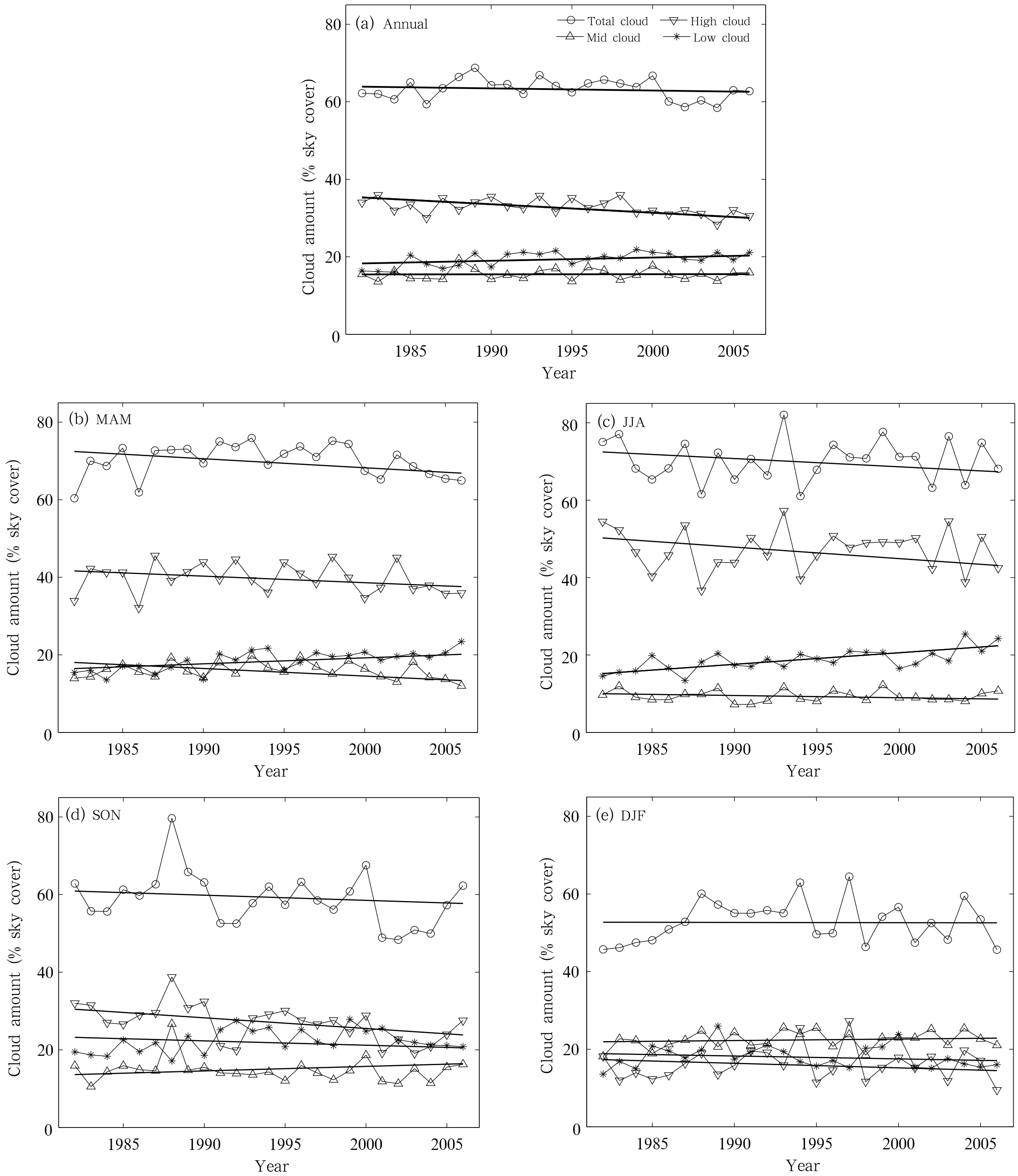

Fig. 4. Time series and linear trends of (a) annual and (b–e) seasonal mean cloud amount from 1982 to 2006, averaged over the Yangtze River Delta. Thick lines indicate trends with significance at the 95% confidence level. (b) Spring: March, April, and May (MAM); (c) Summer: June, July, and August (JJA); (d) Autumn: September, October, and November (SON); (e) Winter: December, January, and February (DJF).

with a decreasing tendency for the past 25 years; and this variation agrees well with the result of surface observations (Yuan and Tang, 2007). The annual mean high-level cloud amount has a statistically significant decreasing trend of –2.2% sky cover per decade, which plays a major role in the decrease of the total cloud amount. The annual mean mid-level clouds have the lowest frequency of occurrence and are the least invariant. The annual mean low-level cloud amount has a unique increasing tendency of 0.8% sky cover per decade.

Variations of seasonal mean cloud amounts are illustrated in Figs. 4b–e. High-level clouds have decreasing tendencies throughout the year while the low-level cloud amount in summer shows a continued growth, with the increasing trend of 3.0% sky cover per decade at the 95% confidence level (Fig. 4c).

The spatial distributions of linear trends in low-level cloud amount during summer are shown in Fig. 5a. The low-level cloud amount increases over the entire YRD and it is notable that the increasing trend over and around most urban areas is higher with relative maxima centers emerging west of Shanghai (SH). The lower trend values are located over Tai Lake with a water area of 2500 km^2 and mountain areas covered by forest (southwest of YRD). Meanwhile, this relative growth directly results in a smaller decrease of total cloud amount over most urban areas (Fig. 5b: from SH to northwest of Changzhou (CZ)). Additionally, the decrease extent of the high-level cloud amount is smaller over the southwest of the YRD (figure omitted) and therefore, the total cloud amount also has a smaller decreasing tendency over the mountain areas (Fig. 5b).

By further exploring the low-level cloudiness variations over different land covers, we compare the differences of low-level cloud amounts in summer between urban agglomerations (black rectangular areas in Fig. 1b) and the adjacent rural areas including cropland (red rectangular areas in Fig. 1b), Tai Lake, and forest, respectively (Fig. 6). Because the observation resolution (0.5°) is greater than the size of most cities in this area, and the urban land cover expanded dramatically in this analysis period, it is hard to obtain observation data over a pure urban area. In our study, the urban cover fraction over each PATMOS-x grid is calculated with 1-km resolution MODIS land use data (Fig. 1b), and the urban-dominant grids (which means a grid with urban cover fraction greater than 50%) are used to represent the trend for urban agglomerations. As for the cropland area, it also includes some urban land use, such as small-size towns or cities, and the urban cover fraction over the selected cropland area is less than 20% in our analysis. It is clearly evident that the low-level cloud amount increased over urban agglomerations at a faster rate than that over non-urban areas. The increasing rate over urban agglomerations is much greater than those over bodies of water and forest, and it is also greater than that over the cropland area. The trend over the cropland is close to that over the urban area. There may be two potential reasons: 1) the urban-dominant grids used in our analysis usually include cropland, and vice versa; 2) the selected cropland areas are near urban

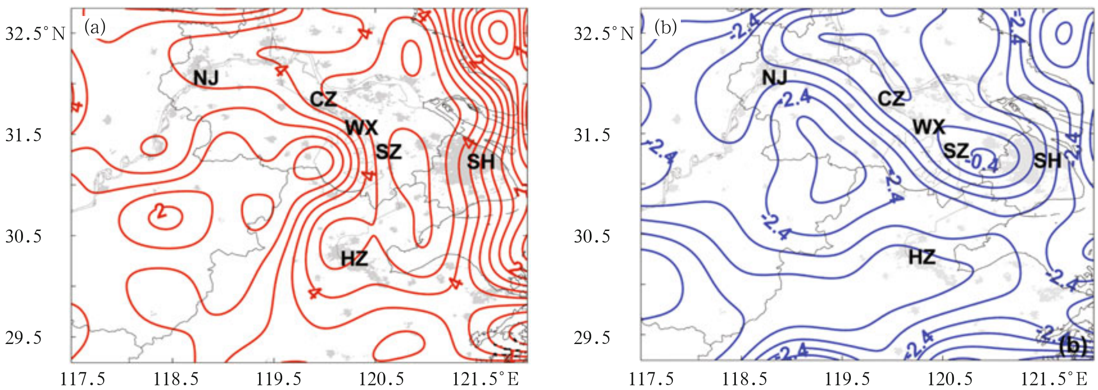

Fig. 5. Trends of summer mean (a) low-level and (b) total cloud amount for 1982–2006 (interval: 0.4% sky cover per decade). The red contour lines indicate increasing trends and blue contour lines indicate decreasing trends. The shaded areas indicate urban areas. NJ: Nanjing; CZ: Changzhou; WX: Wuxi; SZ: Suzhou; SH: Shanghai; HZ: Hangzhou. Trends of low-level clouds are at the 95% confidence level for most of the study areas while trends of total clouds are not significant for any areas.

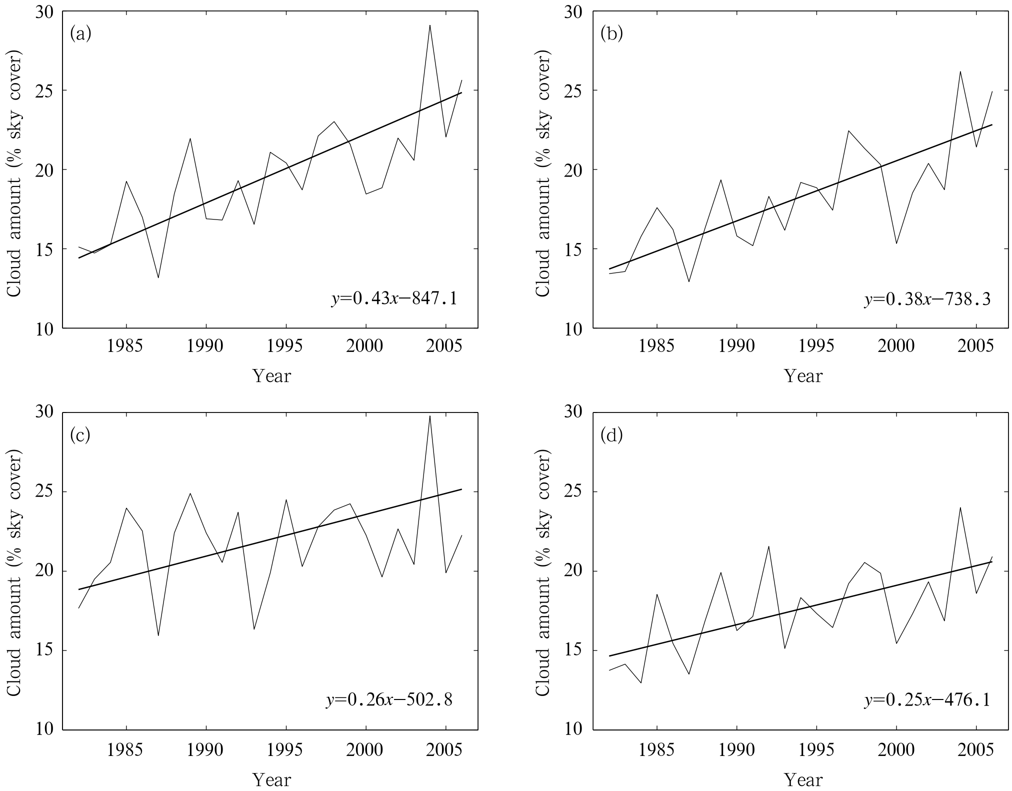

Fig. 6. Changes of low-level cloud amount in summer over (a) urban agglomeration (black rectangular areas in Fig. 1b), (b) cropland (red rectangular areas in Fig. 1b), (c) Tai Lake, and (d) forest areas. Thick lines indicate trends at the 95% confidence level.

agglomerations (Fig. 1b) and the influence of urbanization has a regional-scale impact in this area, as demonstrated by previous studies (e.g., Zhang N. et al., 2010). Further studies with higher resolution observations and state-of-the-art numerical modeling are needed for a better explanation on this phenomenon.

4. Discussion

The cloud process is very complex and impacted by many factors such as moisture, cloud condensation nuclei (CNN), and thermal excitation, especially when considering the adequate water vapor supply from the oceans and densely vegetated land cover in the YRD in summer. The key factors of cloud processes are related to CCN and thermal excitation. The CCN concentration increases due to the air pollutant release over urban area, and its impact on clouds is very uncertain. A large number of studies based on observations and models indicate that high concentrations of fine aerosol particles could increase cloud coverage by increasing the concentration of cloud droplets that not only suppress rainfall in warm cloud but also augment the cloud top albedo (Rosenfeld, 1999, 2000; Givati and Rosenfeld, 2004; Teller and Levin, 2006; Khain et al., 2008; Small et al., 2011). Other studies also find that aerosols could reduce cloud cover as well: for example, hydrophilic aerosols may enhance precipitation in the ice phase and reduce the cloud cover (Lohmann, 2002); absorbing aerosols (black carbon) could heat the atmosphere by absorbing solar radiation, which results in reduced cloud formation and abbreviation of cloud lifetime (Ackerman et al., 2000; Small et al., 2011). All the previous studies show that the effects of aerosols on cloud amount tend to be more on the global scale rather than regional or urban scales.

The most probable mechanism of the low-level cloud increasing over the YRD in summer is the surface heating excitation, especially when this area is currently undergoing rapid urbanization. Urbaninduced modifications in natural clouds may well be due to the following causes (Cotton and Pielke, 2007): 1) increases in anthropogenic aerosols effects; 2) the urban thermal effect on low-level convection and circulation; 3) increased low-level convergence downwind of the urban area caused by greater surface roughness; 4) changes of low-level atmospheric moisture content. In summer, the moisture is transported from the East China Sea to the YRD under the prevailing wind (southeast wind) and the strongest UHI effect also appears in summer over the YRD (Du et al., 2007; Zhang K. X. et al., 2010), which may explain why the relative growth of low-level cloudiness over urban areas is more remarkable during summer.

Many observational studies have proved that the apparent intensity increase of UHI over the YRD reflects the tendency of clusters of urban centers to form a large regional heat island (Chen et al., 2006; Du et al., 2007). Table 2 shows the heat island intensity of three typical cities during summer. It is found that the UHI intensity has dramatically increased since the 1990s over all the three cities, and the correlation coefficient between the UHI intensity of Shanghai and the low-level cloudiness over Shanghai is 0.57 ($p = 0.003$).

Table 2. The UHI intensity (°C) of Shanghai, Hangzhou, and Nanjing during summer

	Shanghai (Zhang K. X. et al., 2010)	Hangzhou (Li et al., 2009)	Nanjing (Qiu et al., 2008)
1980–1989	0.49	0.39	0.34
1990–1999	0.86	0.70	0.51
2000–2006	1.07	1.16	0.46 (2000–2005)

5. Conclusions

Variations of seasonal and annual mean cloud amounts of different cloud types (including total cloud, high-level cloud, mid-level cloud, and low-level cloud) were examined and analyzed over the Yangtze River Delta (YRD), China, for the period 1982–2006 by using a linear regression analysis. For the monthly variations, both total and high-level cloud amounts peak in June and reach a minimum in December. In contrast, mid-level clouds have a peak during winter months and reach a minimum in summer while low-level clouds vary weakly throughout the year. The annual averages of total, high-, mid-, and low-level cloud amounts are 63%, 32%, 15%, and 19%, respectively. A decrease tendency in annual mean total cloud amount is found, which is mainly driven by the decreases of high-level clouds throughout the year. Mid-level cloud amounts occur least and remain invariant throughout the year, while the annual mean low-level cloud increase is mainly caused by the significantly increasing trend in low-level cloud amount during the summer.

In particular, the spatial and temporal variations of total and low-level cloud amounts in summer were further analyzed. Trends in the low-level cloud amount during summer have conspicuous local differences: low-level cloud amount over urban agglomeration areas rises much faster than that over the adjacent non-urban areas. This relative growth directly leads to a smaller decreasing tendency of the total cloud amount as observed over most urban areas (–0.4% sky cover per decade) than that over other non-urban areas (–1.2% to –4% sky cover per decade).

In this study, we just provide the spatiotemporal characteristics of cloud amount over the YRD, and try to infer the possible urbanization thermal effect on the low-level cloud. Given the complexity of the cloud physical progresses, higher resolution observations and numerical simulations will be needed to verify the urbanization effect on clouds, and further quantitative research is warranted to detect more examples of these effects.

Acknowledgments. We are grateful to the anonymous reviewers for their valuable comments.

REFERENCES

Ackerman, A. S., O. B. Toon, D. E. Stevens, et al., 2000: Reduction of tropical cloudiness by soot. *Science*, **288**, 1042–1047, doi: 10.1126/science.288.5468.1042.

Chen, L. X., W. L. Li, W. Q. Zhu, et al., 2006: Seasonal trends of climate change in the Yangtze Delta and its adjacent regions and their formation mechanisms. *Meteor. Atmos. Phys.*, **92**, 11–23, doi: 10.1007/s00703-004-0102-y.

Clement, A. C., R. Burgman, and J. R. Norris, 2009: Observational and model evidence for positive low-level cloud feedback. *Science*, **325**, 460–464, doi: 10.1126/science.1171255.

Cotton, W. R., and R. A. Pielke, 2007: *Human Impacts on Weather and Climate*. Cambridge University Press, New York, 330 pp.

Dong, X., B. Xi, K. Crosby, et al., 2010: A 10 year climatology of arctic cloud fraction and radiative forcing at Barrow, Alaska. *J. Geophys. Res.*, **115**(D17), D12124, doi: 10.1029/2009JD013489.

Du, Y., Z. Q. Xie, Y. Zeng, et al., 2007: Impact of urban expansion on regional temperature change in the Yangtze River Delta. *Journal of Geographical Sciences*, **17**, 387–398, doi: 10.1007/s11442-007-0387-0.

Endo, N., and T. Yasunari, 2006: Changes in low cloudiness over China between 1971 and 1996. *J. Climate*, **19**, 1204–1213, doi: 10.1175/JCLI3679.1.

Givati, A., and D. Rosenfeld, 2004: Quantifying precipitation suppression due to air pollution. *J. Appl. Meteor.*, **43**, 1038–1056, doi: 10.1175/1520-0450(2004)043<1038%3AQPSDTA>2.0.CO%3B2.

Heidinger, A. K., and M. J. Pavolonis, 2009: Gazing at cirrus clouds for 25 years through a split window. Part I: Methodology. *J. Appl. Meteor. Climatol.*, **48**, 1100–1116, doi: 10.1175/2008JAMC1882.1.

Kaiser, D. P., 1998: Analysis of total cloud amount over China, 1951–1994. *Geophys. Res. Lett.*, **25**, 3599–3602, doi: 10.1029/98GL52784.

——, 2000: Decreasing cloudiness over China: An updated analysis examining additional variables. *Geophys. Res. Lett.*, **27**, 2193–2196, doi: 10.1029/2000 GL011358.

Kennedy, A. D., X. Q. Dong, B. K. Xi, et al., 2010: Evaluation of the NASA GISS Single-Column Model simulated clouds using combined surface and satellite observations. *J. Climate*, **23**, 5175–5192, doi: 10.1175/2010JCLI3353.1.

Khain, A. P., N. BenMoshe, and A. Pokrovsky, 2008: Factors determining the impact of aerosols on surface precipitation from clouds: An attempt at classification. *J. Atmos. Sci.*, **65**, 1721–1748, doi: 10. 1175/2007JAS2515.1.

Li, Y., R. Yu, Y. Xu, et al., 2004: Spatial distribution and seasonal variation of cloud over China based on ISCCP data and surface observations. *J. Meteor. Soc. Japan*, **82**, 761–773, doi: 10.2151/jmsj.2004.761.

Li Qiang, Zhou Suoquan, Xiang Liang, et al., 2009: The analysis on temporal-spatial characters of urban agglomeration island effect in Hangzhou Bay. *Bulletin of Science and Technology*, **25**, 395–418. (in Chinese)

Liang, F., and X. A. Xia, 2005: Long-term trends in solar radiation and the associated climatic factors over China for 1961–2000. *Ann. Geophys.*, **23**, 2425–2432, doi: 10.5194/angeo-23-2425-2005.

Lohmann, U., 2002: A glaciation indirect aerosol effect caused by soot aerosols. *Geophys. Res. Lett.*, **29**, 11-1-11-4, doi: 10.1029/2001GL014357.

Nieman, S. J., J. Schmetz, and W. P. Menzel, 1993: A comparison of several techniques to assign heights to cloud tracers. *J. Appl. Meteor.*, **32**, 1559–1568, doi: 10.1175/1520-0450(1993)032<1559: ACOSTT>2.0.CO;2.

Pavolonis, M. J., and A. K. Heidinger, 2004: Daytime cloud overlap detection from AVHRR and VIIRS. *J. Appl. Meteor.*, **43**, 762–778, doi: 10.1175/2099.1.

——, ——, and T. Uttal, 2005: Daytime global cloud typing from AVHRR and VIIRS: Algorithm description, validation, and comparisons. *J. Appl. Meteor.*, **44**, 805–826, doi: 10.1175/JAM2236.1.

Qian, Y., D. P. Kaiser, L. R. Leung, et al., 2006: More frequent cloud-free sky and less surface solar radiation in China from 1955 to 2000. *Geophys. Res. Lett.*, **33**, L01812, doi: 10.1029/2005GL024586.

Qiu Xinfa, Gu Lihua, Zeng Yan, et al., 2008: Study on urban heat island effect of Nanjing. *Climatic Environ. Res.*, **13**, 807–814. (in Chinese)

Randall, D. A., and S. Tjemkes, 1991: Clouds, the earth's radiation budget, and the hydrologic-cycle. *Global and Planetary Change*, **90**, 3–9, doi: 10.1016/0921-8181(91)900633.

Rosenfeld, D., 1999: TRMM observed first direct evidence of smoke from forest fires inhibiting rainfall. *Geophys. Res. Lett.*, **26**, 3105–3108, doi: 10.1029/1999GL006066.

——, 2000: Suppression of rain and snow by urban and industrial air pollution. *Science*, **287**, 1793–1796, doi: 10.1126/science.287.5459.1793.

Rossow, B. R., and R. A. Schiffer, 1999: Advances in understanding clouds from ISCCP. *Bull. Amer. Meteor. Soc.*, **80**, 2261–2287, doi: 10.1175/1520-0477(1999)080<2261:AIUCFI>2.0.CO;2.

Small, J. D., J. H. Jiang, H. Su, et al., 2011: Relationship between aerosol and cloud fraction over Australia. *Geophys. Res. Lett.*, **38**, L23802, doi: 10.1029/2011GL049404.

Tang, Q. H., G. Y. Leng, and P. Y. Groisman, 2012: European hot summers associated with a reduction of cloudiness. *J. Climate*, **25**, 3637–2644, doi: 10.1175/JCLI-D-12-00040.1.

Teller, A., and Z. Levin, 2006: The effects of aerosols on precipitation and dimensions of subtropical clouds: A sensitivity study using a numerical cloud model. *Atmos. Chem. Phys.*, **6**, 67–80, doi: 10.5194/acp-6-67-2006.

Thomas, S. M., A. K. Heidinger, and M. J. Pavolonis, 2004: Comparison of NOAA's operational AVHRR-derived cloud amount to other satellite-derived cloud climatologies. *J. Climate*, **17**, 4805–4822, doi: 10.1175/JCLI-3242.1.

Tiao, G. C., G. C. Reinsel, D. M. Xu, et al., 1990: Effects of autocorrelation and temporal sampling schemes on estimates of trend and spatial correlation. *J. Geophys. Res.*, **95**(D12), 20507–20517.

Warren, S. G., R. M. Eastman, and C. J. Hahn, 2007: A survey of changes in cloud cover and cloud types over land from surface observations, 1971–96. *J. Climate*, **20**, 717–738, doi: 10.1175/JCLI4031.1.

Weatherhead, E. C., G. C. Reinsel, G. C. Tiao, et al., 1998: Factors affecting the detection of trends: Statistical considerations and applications to environmental data. *J. Geophys. Res.*, **103**(D14), 17149–17161.

Xi, B., X. Dong, P. Minnis, et al., 2010: A 10 year climatology of cloud cover and vertical distribution derived from both surface and GOES observations over the DOE ARM SGP Site. *J. Geophys. Res.*, **115**(D12), D12124, doi: 10.1029/2009JD012800.

Yuan Changhong and Tang Jianping, 2007: Regional climatic response of Jiangsu to global warming. *Journal of Nanjing University (Natural Sciences)*, **43**, 655–669. (in Chinese)

Zhang, K. X., R. Wang, C. C. Shen, et al., 2010: Temporal and spatial characteristics of the urban heat island during rapid urbanization in Shanghai, China. *Environ. Monit. Assess.*, **169**, 101–112, doi: 10.1007/s10661-009-1154-8.

Zhang, N., Z. Q. Gao, X. M. Wang, et al., 2010: Modeling the impact of urban ization on the local and regional climate in Yangtze River Delta, China. *Theor. Appl. Climatol.*, **102**, 331–342, doi: 10.1007/s00704-010-0263-1.

Zhang, Y. L., B. Q. Qin, and W. M. Chen, 2004: Analysis of 40 year records of solar radiation data in Shanghai, Nanjing and Hangzhou in eastern China. *Theor. Appl. Climatol.*, **78**, 217–227, doi: 10.1007/s00704-003-0030-7.